

Xu Deng^{1,2*} and Sarah E. Perkins-Kirkpatrick^{1,2}

¹School of Science, University of New South Wales, Canberra, ACT, Australia.

²ARC Centre of Excellence for Climate Extremes, University of New South Wales, Canberra, ACT, Australia.

Corresponding author: Xu Deng (xu.deng@student.adfa.edu.au)

Key Points:

- There indicates a “warm-get-warmer” pattern for some extremes over Australia and tropical regions usually show the highest warming
- Compared to CMIP5, the higher warming for some extremes in CMIP6 can lead to earlier time of emergence under the highest scenario
- Internal variability influences the determination of the noise

Abstract

This study focuses on the projections and time of emergence (TOE) for temperature extremes over Australian regions in the phase 6 of Coupled Model Intercomparison Project (CMIP6) models. The model outputs are based on the Shared Socioeconomic Pathways (SSPs) from the Tier 1 experiments (i.e., SSP1-2.6, SSP2-4.5, SSP3-7.0 and SSP5-8.5) in the Scenario Model Intercomparison Project (ScenarioMIP), which is compared with the Representative Concentration Pathways (RCPs) in CMIP5 (i.e., RCP2.6, RCP4.5 and RCP8.5). Furthermore, two large ensembles (LEs) in CMIP6 are used to investigate the effects of internal variability on the projected changes and TOE. As shown in the temporal evolution and spatial distribution, the strongest warming levels are projected under the highest future scenario and the changes for some extremes follow a “warm-get-warmer” pattern over Australia. Over subregions, tropical Australia usually shows the highest warming. Compared to the RCPs in CMIP5, the multi-model medians in SSPs are higher for some indices and commonly exhibit wider spreads, likely related to the different forcings and higher climate sensitivity in a subset of the CMIP6 models. Based on a signal-to-noise framework, we confirm that the emergence patterns differ greatly for different extreme indices and the large uncertainty in TOE can result from the inter-model ranges of both signal and noise, for which internal variability contributes to the determination of the signal. We further demonstrate that the internally-generated variations influence the noise. Our findings can provide useful information for mitigation strategies and adaptation planning over Australia.

1 Introduction

Anthropogenic climate change will lead to more severe temperature extremes, which have significant impacts on society and natural systems (Intergovernmental Panel on Climate Change, 2021). To assess possible climate futures, projections by global climate models from the Scenario Model Intercomparison

Project (ScenarioMIP; O'Neill et al., 2016) as part of the Coupled Model Inter-comparison Project phase 6 (CMIP6; Eyring et al., 2016) are useful resources, and may provide new insights into how temperature extremes are projected to change under climate change (e.g., Alexander & Arblaster, 2017; Grose et al., 2020; Sillmann, Kharin, Zwiers, et al., 2013; Thibeault & Seth, 2014).

Over Australia, Alexander and Arblaster (2017) indicated that significant increases (decreases) are projected for the occurrence of warm (cold) extremes by the end of this century under the intermediate- and highest-emission scenarios in CMIP5, and that these changes are most distinct in the tropics. Compared to 29 CMIP5 models, Grose et al. (2020) documented that projected changes in temperature extremes over Australia are more distinct and span narrower ranges in seven CMIP6 models. However, the smaller number of models used in this study may lead to misleading conclusions. Recently, Tebaldi et al. (2021) demonstrated that the CMIP6 ensemble projects higher warming and larger spread for global mean temperature compared with CMIP5, which could result from both a wider range of radiative forcing and higher climate sensitivity in a subset of CMIP6 models. In the present study, to obtain a more reasonable comparison with CMIP5, more models are included in the CMIP6 ensemble to analyze the projected changes of temperature extremes over Australia.

In addition, detecting the time of emergence (TOE) for extremes over Australia needs investigation. TOE is defined as the time when the externally forced climate signal (i.e., forced response) emerges from the noise (i.e., natural variability), suggesting that a significant change is detected and a novel climate regime become evident (e.g., Hawkins et al., 2020; Hawkins & Sutton, 2012; King, Donat, et al., 2015). Estimating TOE can provide insights for mitigation strategies, adaptation planning and scientific community, as the forced response relative to the background noise may be more relevant for the assessment of climate impacts, compared to the absolute change (Beaumont et al., 2011; Deutsch et al., 2008; Hawkins et al., 2020; Hawkins & Sutton, 2012; Ossó et al., 2021). For example, similar absolute changes in extreme temperature can result in different ecological impacts since extratropical ecosystems are usually more resilient than tropical ecosystems, as they are adapted to a more variable climate (Beaumont et al., 2011; Deutsch et al., 2008).

Previous studies have concluded that for mean temperature there is earlier TOE over tropical regions than that in the extratropics where the noise is generally larger (e.g., Giorgi & Bi, 2009; Hawkins et al., 2020; Hawkins & Sutton, 2012; Mahlstein et al., 2012; Mahlstein et al., 2011). Furthermore, for warm and cold extremes that display larger variability, the signals for these indices tend to emerge later over both the tropics and extratropics (e.g., King, Donat, et al., 2015; Tan et al., 2018) relative to mean temperature. Currently, most studies on TOE have been conducted at global levels, with less detailed analyses over smaller-scale regions (e.g., Batibeniz et al., 2020; Gaetani et al., 2020; Ossó et al., 2021), especially for Australia (King, Donat, et al., 2015). Under different future scenarios, we aim to investigate the TOE of extreme temperatures over

Australia at the subregional scale.

A variety of methods have been used in TOE assessment, which can lead to a source of uncertainty (Abatzoglou et al., 2019; Gaetani et al., 2020). A recent study (Gaetani et al., 2020) found that compared to Kolmogorov-Smirnov (KS) non-parametric test (King, Donat, et al., 2015), the signal-to-noise ratio (SNR) frameworks exhibit increased uncertainty and later times for TOE over West Africa (Gaetani et al., 2020). However, the SNR methods facilitate the separation between signal and noise, and identifying both components and their interaction physically (e.g., slow-varying ocean conditions and the modes of internal variability) can deepen our understanding in climate change (e.g., Barnes et al., 2019; Barsugli & Battisti, 1998). In this study, we adopt the method by Hawkins and Sutton (2012) and Hawkins et al. (2020) to address the TOE assessment, which is widely used and allows more cross-study comparisons (e.g., Abatzoglou et al., 2019; Gaetani et al., 2020; Hawkins et al., 2020; Hawkins & Sutton, 2012; Ossó et al., 2021). For the uncertainty in the detection of TOE in this method, it can arise from inter-model spread not only in the signal, but also from noise (Hawkins & Sutton, 2012).

Furthermore, as internal variability can also be an important source of uncertainty for regional climate (Dai & Bloecker, 2019; Deser, Knutti, et al., 2012; Deser, Phillips, et al., 2012; Hawkins & Sutton, 2009; Lehner et al., 2020), single-model initial-condition large ensembles (SMILEs; hereafter LEs) are an important tool to investigate the consequences of the intrinsic variability on the uncertainty in projected changes and TOE of extreme temperatures over Australia, of which external forcing and model structure are identical among the members (e.g., Dai & Bloecker, 2019; Deser, 2020; Deser et al., 2020; Lehner et al., 2020; Mankin et al., 2020; Perkins-Kirkpatrick et al., 2017; Xie et al., 2015).

Previous research evaluated the ability of CMIP6 models to simulate extreme temperatures over Australian regions in the historical period (1950-2014), compared these results to the CMIP5 ensemble, and investigated the effects of internal variability on the corresponding trends based on the LEs in CMIP6 (Deng et al., 2021). Following from this research, the purposes of this study are: to assess future climate changes of the extremes and the TOE over Australian regions in both the CMIP6 and CMIP5 models, and to explore the effects of internal variability on the projected changes and TOE based on LEs in CMIP6.

2 Data and Methods

2.1 Model Data

Although the scenarios in the ScenarioMIP consist of two tiers, we only use the Tier 1 experiments based on the Shared Socioeconomic Pathway (SSP) scenarios: SSP1-2.6, SSP2-4.5, SSP3-7.0 and SSP5-8.5, as these sample a varying range of possible emission futures and contain relatively large number of model outputs. Among them, SSP1-2.6, SSP2-4.5 and SSP5-8.5 indicate the same nominal stratospheric-adjusted radiative forcing (2.6, 4.5 and 8.5 W m^{-2}) reached in 2100, compared to the scenarios based on Representative Concentration Path-

ways (RCPs) used in CMIP5 (i.e., RCP2.6, RCP4.5 and RCP8.5); and SSP3-7.0 fills a gap between medium and high end in the range of future forcing pathways, not included in previous CMIP generations (O'Neill et al., 2016; Tebaldi et al., 2021). Despite the similarity among the future scenarios in CMIP6 and CMIP5, it is noted that there are some differences, such as the composition of some radiatively active gases or species (e.g., CO₂ and CH₄) and aerosol emissions, making the resulting effective radiative forcing (ERF) different (Lurton et al., 2020; Riahi et al., 2017; Tebaldi et al., 2021).

As one aim of this study is to compare the two CMIP ensembles in projected changes and TOE in extremes, we do not consider the interdependence among the models and use emergent constraints or any other ways of model weighting to reduce the differences between CMIP6 and CMIP5 (e.g., Tokarska et al., 2020), which is similar to the practice by Seneviratne and Hauser (2020). Similar to Deng et al. (2021), only one ensemble member (typically the first member) in each model is considered for the main part of analysis. There are 25 models in CMIP6 and 26 models in CMIP5 for at least one of the future scenarios. In addition, two LEs under SSP5-8.5 and SSP1-2.6 in CMIP6 are used to investigate the impacts of internal variability on the projected changes and TOE of the extremes: CanESM5-LE and MIROC6-LE, which contain 25 members and 50 members, respectively. Detailed information on the simulations from CMIP6 and CMIP5 models are listed in the Tables S1 and S2, respectively.

2.2 Temperature indices

As in Deng et al. (2021), based on daily maximum and minimum temperatures (TX and TN), the annualized temperature extremes defined by the Expert Team on Climate Change Detection and Indices (ETCCDI; Zhang et al., 2011) are used, which forms a continuous and comprehensive investigation of changes in extremes, similar to other studies for CMIP5 (e.g., Alexander & Arblaster, 2017; Sillmann, Kharin, Zhang, et al., 2013; Sillmann, Kharin, Zwiers, et al., 2013; Thibeault & Seth, 2014). Besides diurnal temperature range (DTR), other extreme indices for temperatures are classified into four categories: absolute indices (hottest day [TXx], coldest day [TXn], warmest night [TNx] and coldest night [TNn]), threshold indices (summer days [SU], tropical nights [TR] and frost days [FD]), percentile-based indices (warm days [TX90p], cold days [TX10p], warm nights [TN90p] and cold nights [TN10p]), and duration indices (warm spell duration index [WSDI] and cold spell duration index [CSDI]). The bootstrap resampling procedure by Zhang et al. (2005) is applied to the percentile-based and duration indices, among which the spells crossing year boundaries are taken into consideration for WSDI and CSDI. Since the definitions of growing season length (GSL) and ice days (ID) are not suitable over most of Australia (Alexander & Arblaster, 2017), we do not use them in this study. Detailed information on the indices can be found in Table S3.

2.3 Time of Emergence

The TOE is determined using the signal-to-noise framework as detailed by

Hawkins and Sutton (2012) and Hawkins et al. (2020), which is considered as the first year when the signal-to-noise ratio (SNR) is larger than nominated thresholds (e.g., 1 and 2). As suggested by Frame et al. (2017), we consider SNR=1 as the threshold for an “unusual” climate and SNR=2 as “unfamiliar”. This approach linearly regresses annual local variations in temperature extremes onto global mean surface temperature change ($GMST$), relative to the base period:

$$\widehat{L}(t) = \alpha G(t) + \beta$$

where $\widehat{L}(t)$ represents the regressed $L(t)$, denoting annual local changes in extremes over time; $G(t)$ is a smoothed version of $GMST$ over the same period; α defines the linear scaling between $\widehat{L}(t)$ and $G(t)$; and β is a constant. $GMST$ is smoothed with a “Locally Weighted Scatterplot Smoothing” filter (LOWESS; Cleveland, 1979) of 21 years, which filters out interannual variability (though retaining multi-decadal variability). The signal of local climate change described by $GMST$ is $G(t)$, and the noise is defined as the standard deviation of the residuals ($L(t) - G(t)$). The method implies that local variations for some variables scale well with $GMST$ (Fischer et al., 2014; Seneviratne & Hauser, 2020; Sutton et al., 2015). It is also noted that internal variability can contribute to the determination of signal, which may introduce further uncertainty in the estimate of TOE (Gaetani et al., 2020; Kumar & Ganguly, 2018; Lehner et al., 2020).

To compare observed SNR with the simulations, Berkeley Earth Surface Temperatures (BEST; Rohde, Muller, Jacobsen, Muller, et al., 2013; Rohde, Muller, Jacobsen, Perlmutter, et al., 2013) is used in this study. Although TN in BEST is biased over Australia (Deng et al., 2021), the TX and TN in BEST show higher correlation compared to Australian gridded climate data (AGCD, previously termed Australian Water Availability Project [AWAP]; Jones et al., 2009), which is better than other global datasets, including National Centers for Environmental Prediction/National Center for Atmospheric Research (NCEP/NCAR) Reanalysis 1 (NCEP1; Kalnay et al., 1996), NCEP/Department of Energy (DOE) Reanalysis 2 (NCEP2; Kanamitsu et al., 2002), Twentieth Century Reanalysis (20CR; Compo et al., 2011), and European Centre for Medium-Range Weather Forecasts (ECMWF) Reanalysis version 5 (ERA5) with preliminary extension to 1950 (Bell et al., 2021; Hersbach et al., 2020) (not shown).

2.4 Regional Assessment

According to climatological and geographical conditions (Perkins et al., 2014; http://www.bom.gov.au/climate/change/about/temp_timeseries.shtml), Australia is divided into nine sub-regions: AUS (Australia), NA (Northern Australia), SA (Southern Australia), SEA (South East Australia), MEA (Middle Eastern Australia), TA (Tropical Australia), SWA (South West Australia), SSA (Southern South Australia), CAU (Central Australia), and MWA (Mid-Western

Australia), shown in Table S4 and Fig. S1, which allows a detailed assessment over smaller subregions. And the base period is from 1961 to 1990, which is commonly used and allows us to analyze TOE with respect to a recent period. Still, we regrid TX and TN to $1^\circ \times 1^\circ$ resolution using bilinear interpolation, and then calculate extreme indices. In addition, grid boxes containing less than 75% land are masked out (King, van Oldenborgh, et al., 2015).

In the next section, temporal variations from 1950 to 2100 for the ETCCDI indices in different future scenarios are first analyzed, followed by the spatial patterns of the changes in the indices over 2071-2011 and 2031-2060. Then, the SNR and TOE for TXx and TNn is calculated to address when a novel climate for temperature extremes emerges. For consistency among CMIP6, CMIP5 and BEST, we calculate the noise in SNR for the period 1950-2005, as the estimation of noise can stabilize over longer timescale (Dai & Bloecker, 2019; Santer et al., 2011). Finally, we use two LEs to check the effects of internal variability on the projected responses of extremes and TOE.

3 Results

3.1 Projected changes

Relative to the base period 1961-1990, Figs. 1 and 2 indicate time series of the anomalies for the 14 ETCCDI indices averaged over Australia (10-45°S, 110-155°E) during the period 1950-2100 under different future scenarios in CMIP6 (SSP1-2.6, SSP2-4.5, SSP3-7.0 and SSP5-8.5) and CMIP5 (RCP2.6, RCP4.5 and RCP8.5). For the multi-model medians (Fig. 1), consistent with RCPs in CMIP5 (Fig. 2), the Tier 1 experiments in ScenarioMIP show projected increases in the absolute indices (TXx, TXn, TNx and TNn) and in the warm extremes for percentile-based, duration and threshold indices (TX90p, TN90p, WSDI, SU and TR); in contrast, there are decreases in other cold extremes (TX10p, TN10p, CSDI and FD).

Among the scenarios, the indices under SSP5-8.5 and RCP8.5 generally show larger warming evolution, especially by the end of the century. Moreover, except for DTR, CSDI and FD (Fig. 1e, k and n), extremes under the SSP3-7.0 fill the gap between SSP2-4.5&RCP4.5 and SSP5-8.5&RCP8.5. For example, in the year 2100, the median of TXx under SSP3-7.0 is 4.58°C, lower than 5.78°C&5.82°C in SSP5-8.5&RCP8.5 and higher than 3.24°C&2.67°C in SSP2-4.5&RCP4.5. In the lower emission scenarios (SSP1-2.6&RCP2.6) there is a stabilization for the extremes in the second half of 21st century, achieving lowest warming (e.g., 2.23°C&1.92°C for TXx in 2100). This result implies the benefits of mitigation strategies associated with these scenarios (O'Neill et al., 2016). However, the separation for the adjacent pathways (e.g., SSP5-8.5&SSP3-7.0, SSP3-7.0&SSP2-4.5 and SSP2-4.5&SSP1-2.6) usually occurs after 2060s for most indices over Australia. In particular, compared to SSP5-8.5&RCP8.5, if a more aggressive mitigation policy is undertaken (e.g., SSP1-2.6&RCP2.6), it may still take one or two decades to notice its effects on projected changes in temperature extremes over Australia.

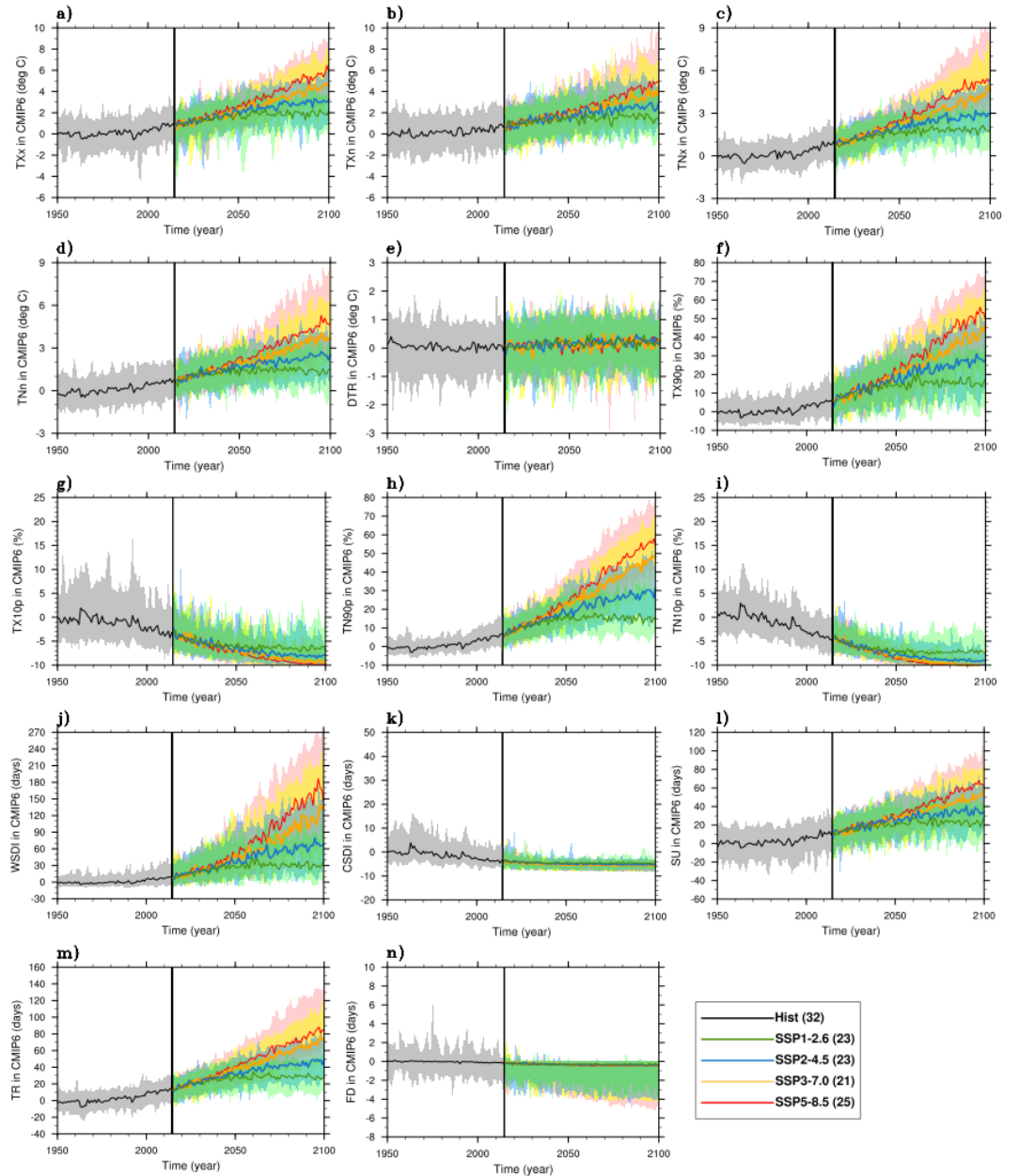


Figure 1. Time series of the anomalies (base period: 1961-1990) for the 14 ETCCDI indices averaged over Australia (10°S – 45°S , 110°E – 155°E) from 1950 to 2100, under the historical simulations and Tier 1 experiments of ScenarioMIP in CMIP6: Hist (grey), SSP1-2.6 (green), SSP2-4.5 (blue), SSP3-7.0 (yellow) and SSP5-8.5 (red) (the number of models indicated in parentheses in the legend). Solid lines represent the multi-model medians and shading indicates the full

range across the models for each experiment.

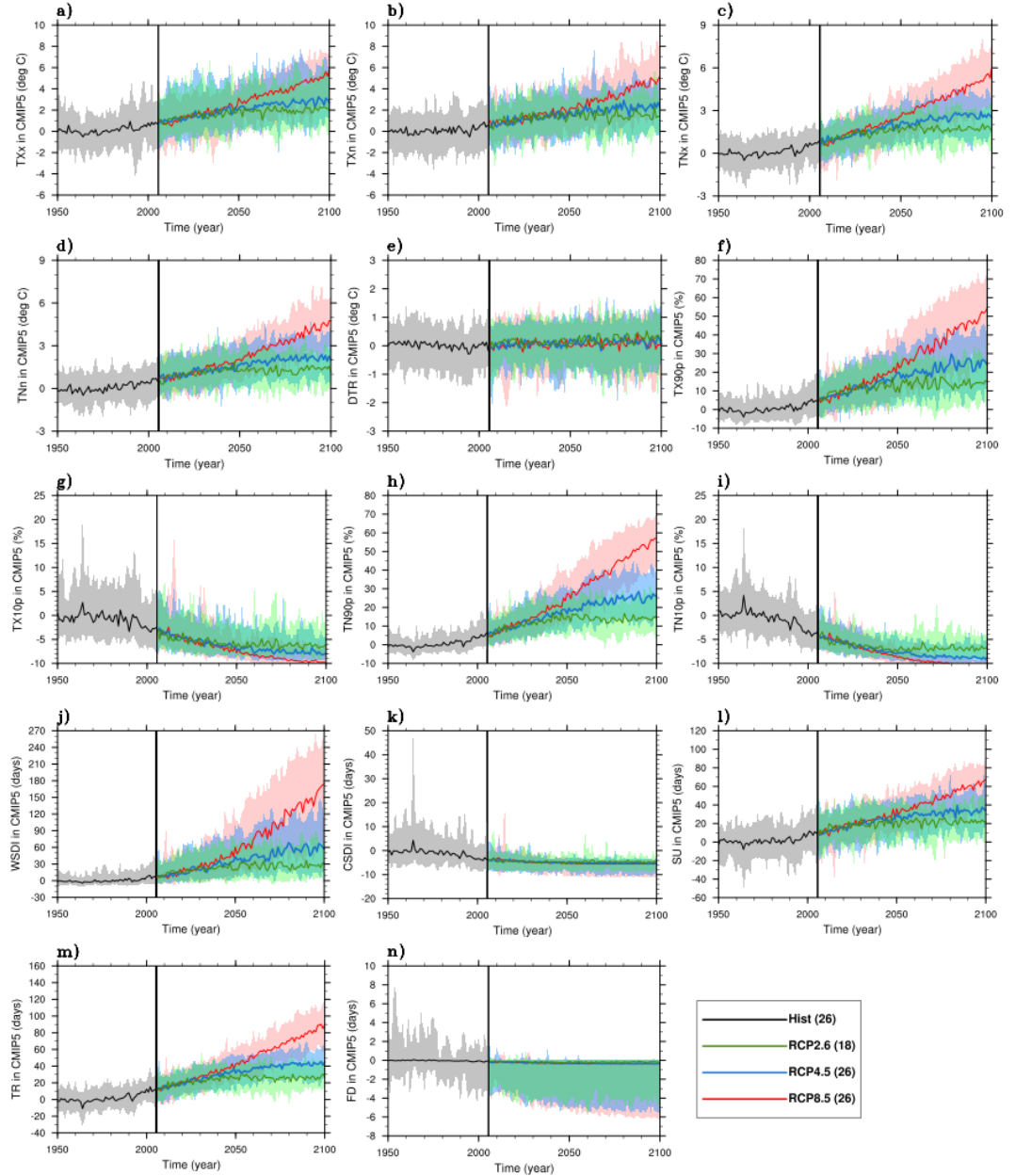


Figure 2. Same as Fig.1, but for CMIP5: Hist (grey), RCP2.6 (green), RCP4.5 (blue), and RCP8.5 (red).

To illustrate the spreads and medians of the projected climatological changes in extremes over Australian regions in detail, boxplots for SSP5-8.5&RCP8.5

and SSP1-2.6&RCP2.6 are shown in Figs. 3 and 4, and Figs. S2 and S3 for SSP3-7.0 and SSP2-4.5&RCP4.5. Over the regions, the spreads of the indices in SSPs and RCPs tend to be larger with higher emission pathways and over time, among which some regions such as NA and TA commonly span relatively wider ranges. Compared to RCP8.5, the spreads in SSP5-8.5 are usually larger, especially over the period 2071-2100. As for the multi-model medians, most indices display larger warming trends over TA and lower warming over southern Australian regions (e.g., SSA and SWA); while for other indices (e.g., TXx, TNx and TN10p), there are relatively similar warming levels across the 10 regions. Relative to RCPs, the warming levels for some indices (e.g., TXx, TNn, and WSDI) tends to be higher under the SSPs; in contrast, the relative magnitudes of some indices between RCPs and SSPs, such as TXn and TNx (e.g., Fig. 3b, c and Fig. S3b, c), differ among the regions and the levels of radiative forcing.

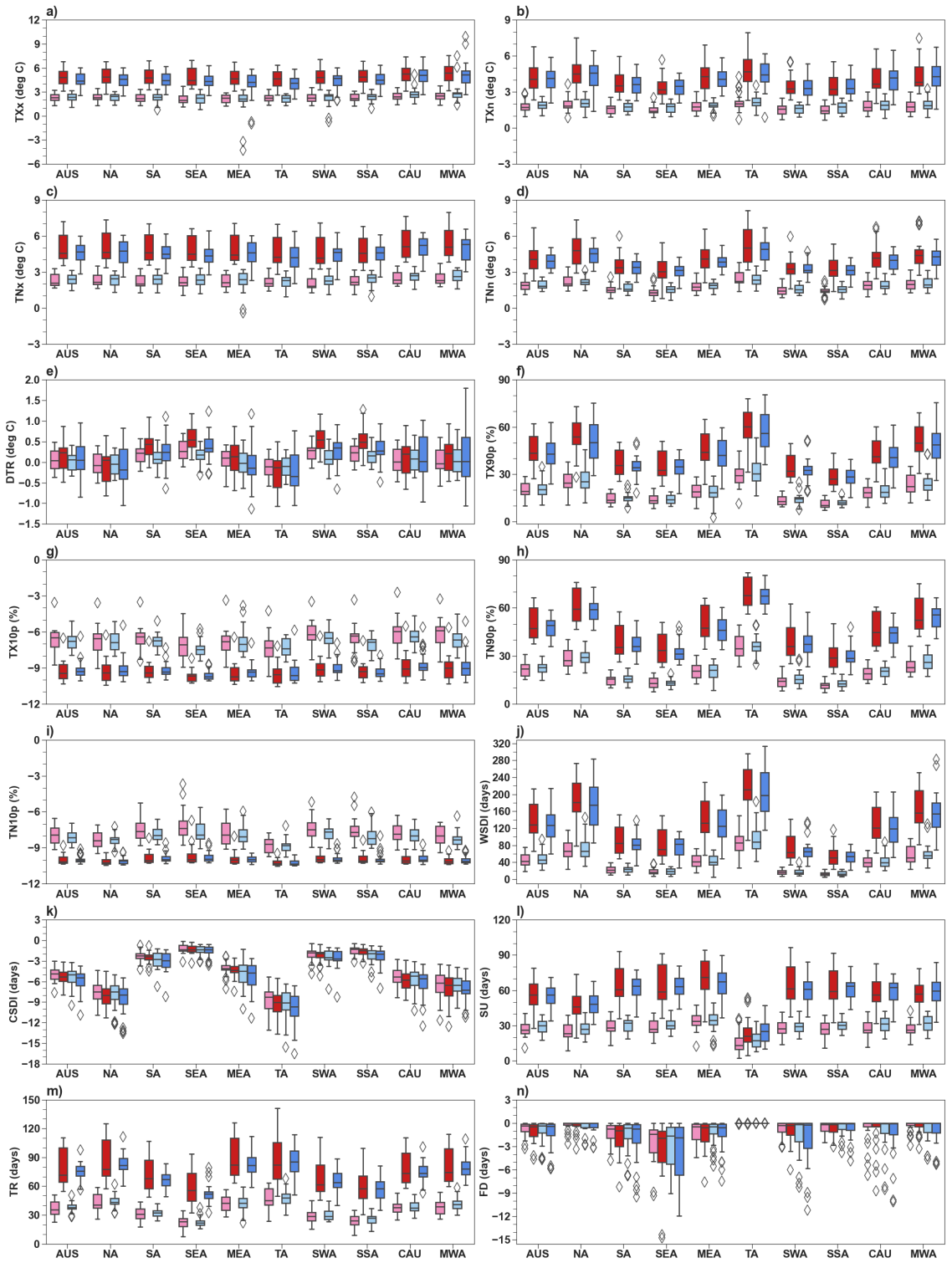


Figure 3. Boxplots of projected changes in the 14 ETCCDI indices over 2071–2100 (bold color) and 2031–2060 (light color) relative to the base period 1961–1990 across 10 Australian regions, under SSP5-8.5 (red) and RCP8.5 (blue). The boxes indicate the interquartile spreads (ranges between the 25th and 75th percentiles), the black lines within the boxes are the multi-model medians, the whiskers extend to the edges of $1.5 \times$ interquartile ranges and “outliers” outside of the whiskers are denoted by diamonds.

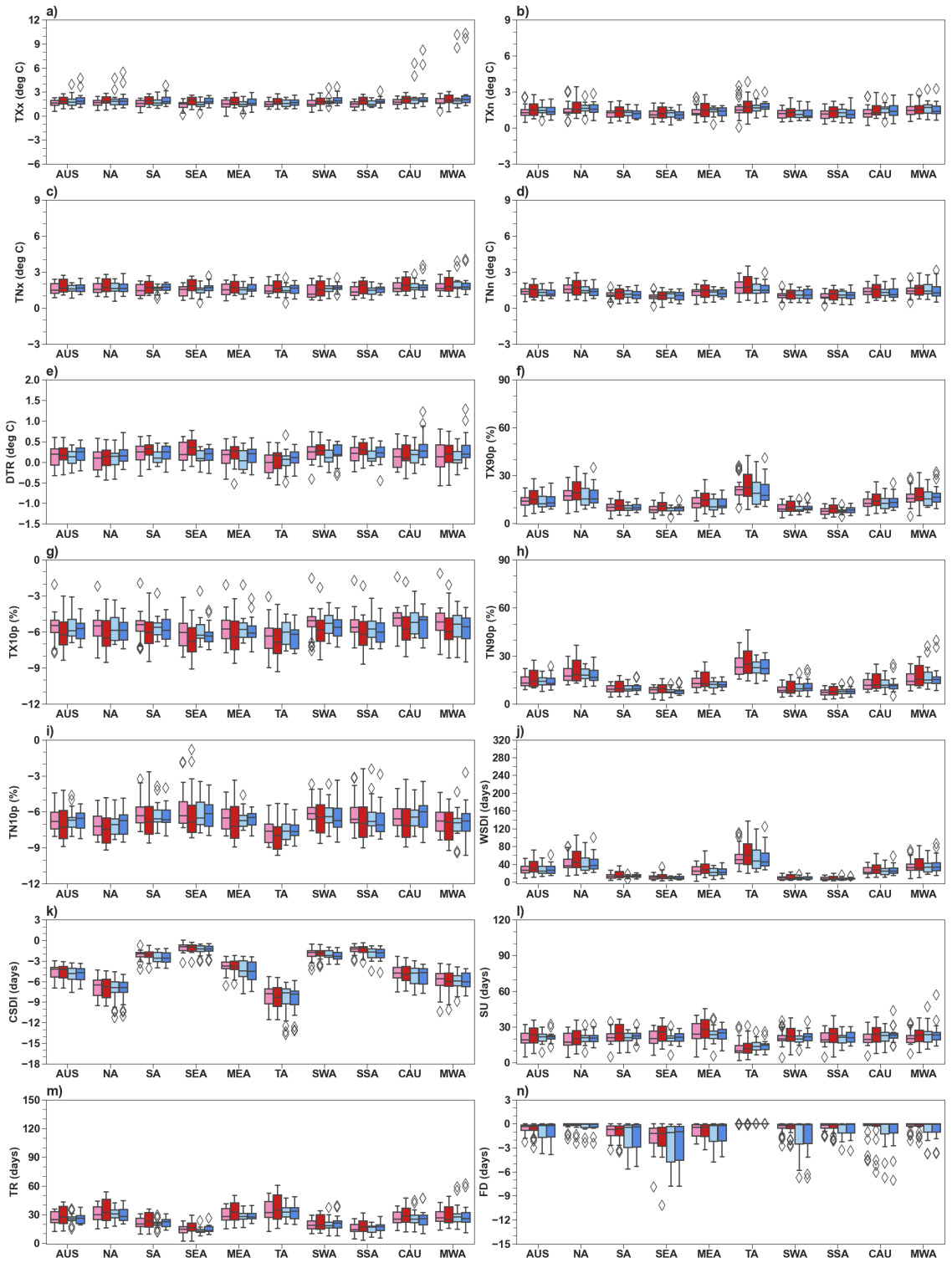


Figure 4. Same as Fig. 3, but for SSP1-2.6 and RCP2.6.

Generally, the spatial patterns for the extremes in both CMIP6 and CMIP5 (Figs. 5 and 6; Figs. S4-S15 in the supplementary material) are similar to previous studies (Alexander & Arblaster, 2017). In the highest scenarios for CMIP6 and CMIP5, the extreme indices show a warmer Australia than other pathways, especially in the end of this century. For most indices (except DTR in Fig. S6 and FD in Fig. S15), most models (at least 75%) in both CMIP ensembles project significant changes in extreme temperature indices over most regions of Australia, both in the middle and the end of the century. However, there are different warming patterns for some indices. For example, as shown in Fig. 5, the warming pattern in TXx is relatively consistent among the regions, with the highest warming over central Australia; while for TNn, Northern Australia displays the most marked warming (Fig. 6).

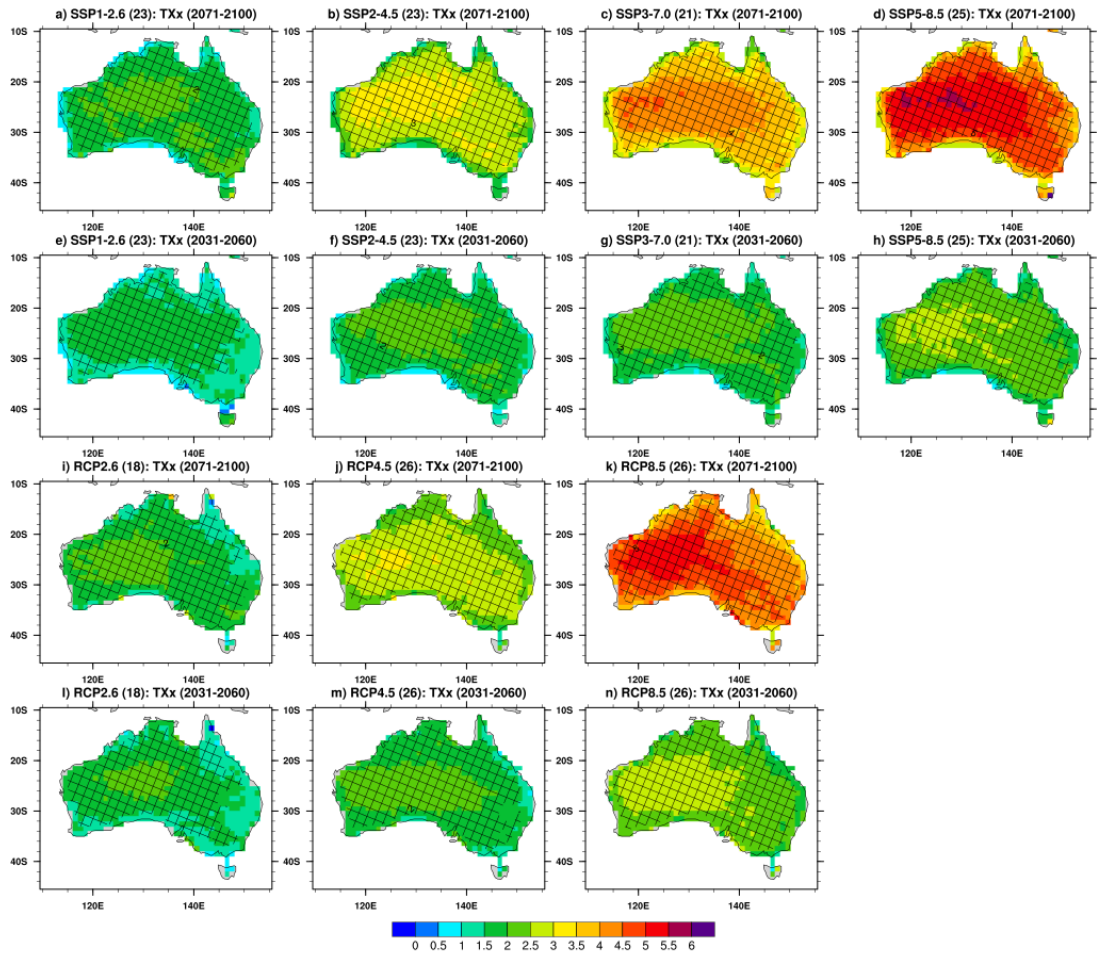


Figure 5. Multi-model median changes in TXx for 2071–2100 (a-d; i-k) and 2031–2060 (e-h; l-n) relative to the base period 1961–2010, under different future scenarios in CMIP6 (SSP1-2.6, SSP2-4.5, SSP3-7.0 and SSP5-8.5) and CMIP5 (RCP2.6, RCP4.5 and RCP8.5). Hatching indicates that at least 75% of the models for each future scenario project significant changes at 95% level, based on the two-tailed Student’s t-test.

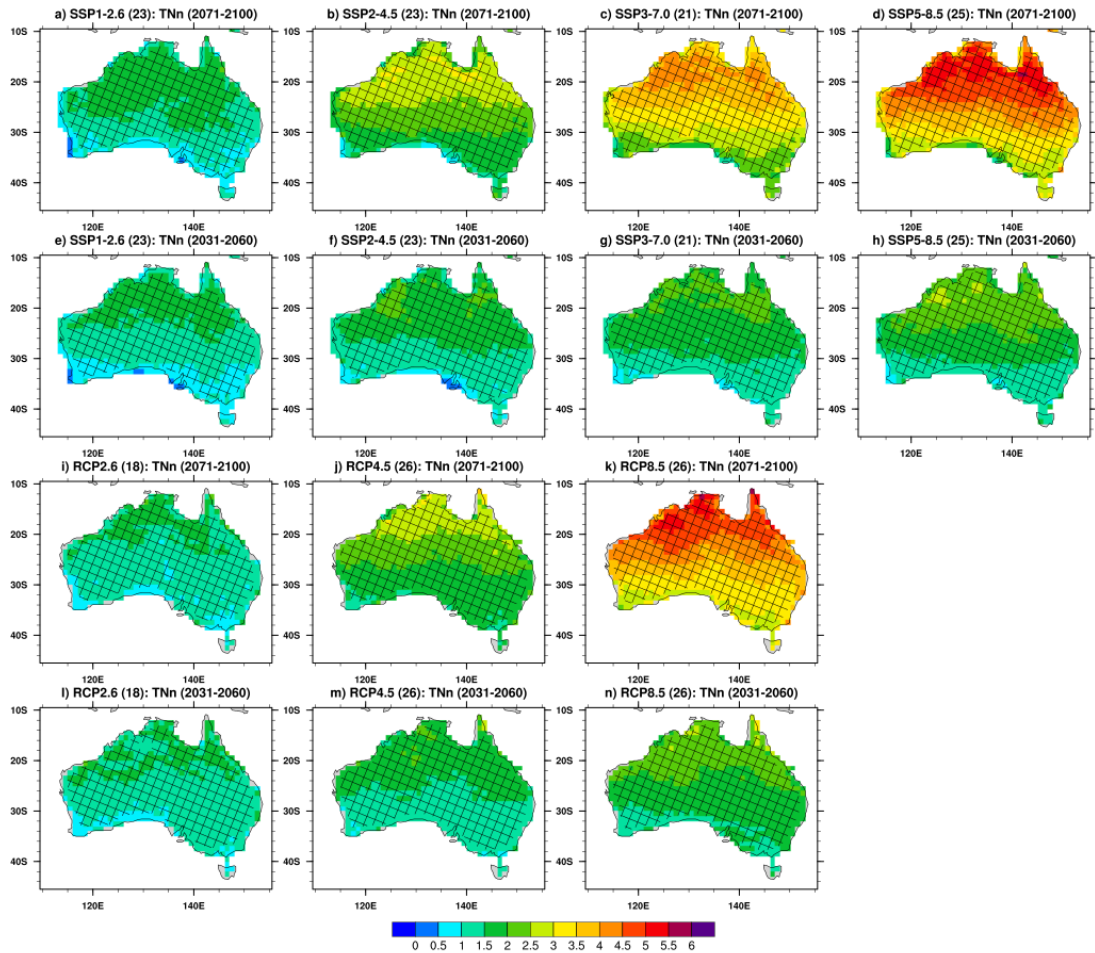


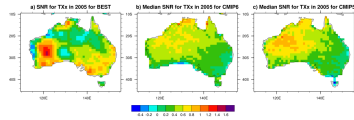
Figure 6. Same as Fig. 5, but for TNn.

Compared to RCP scenarios in CMIP5, the higher projected warming for some extremes (e.g., TXx and TNn) and the larger spreads in CMIP6 (especially under SSP5-8.5) by the end of the 21st century is likely related to the different forcings in the SSPs and higher ECS in some CMIP6 models (e.g., Fyfe et al., 2021; Palmer et al., 2021; Tebaldi et al., 2021). Although there are similar levels of stratospheric-adjusted radiative forcing in 2100 in RCPs and SSPs, aerosol emissions, the composition of gases and some radiatively active species (e.g., CO₂ and CH₄) and the resulting ERF in the pathways can be very different (Fyfe et al., 2021; Lurton et al., 2020; Smith et al., 2020; Tebaldi et al., 2021). In

addition, the wider inter-model spread of the projected changes under stronger external forcing can result from higher climate sensitivity (Lehner et al., 2020; Tebaldi et al., 2021). As documented in Meehl et al. (2020), 12 of the 39 CMIP6 models show higher ECS than the CMIP5 models, some of which can contribute to the wider ranges of projected changes in this study.

3.2 Signal-to-Noise Ratio and Time of Emergence

The maps of SNR for TXx and TNn in the year 2005 are plotted for BEST, CMIP6 and CMIP5 (Fig. 7), the corresponding signal and noise of which are shown in Figs. S16 and S17, respectively. Although the spatial patterns of noise are relatively similar (Fig. S17), the signals of TXx and TNn show noticeable differences between the observation and the two CMIP ensembles (Fig. S16), which means the resulting SNR in BEST and the two CMIP ensembles differ greatly (Fig. 7). The largest observed SNR for TXx (> 1.2) occurs over central and southwestern regions (Fig. 7a), and for TNn there exhibit negative SNR values (< -0.2) over southwest, northern and southeast parts in Australia (Fig. 7d). In contrast, the SNR of TXx and TNn for both CMIP6 and CMIP5 in 2005 tend to be between 0.2 and 0.8. Although there are differences in the observations and the simulations, the low SNR values in 2005 suggest that the signal for the two temperature extremes over most Australia regions has not emerged from the noise.



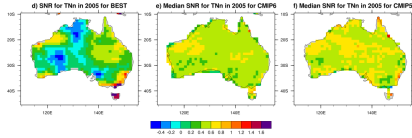


Figure 7. Signal-to-noise ratio (SNR) in the year 2005 for temperature extremes in BEST, CMIP6 and CMIP5. (a) SNR in TX_x for BEST; (b) SNR in TX_x for the multi-model medians in CMIP6; and (c) SNR in TX_x for the multi-model medians in CMIP5. (d-f) Same as (a-c), but for TN_n.

As spatial aggregation or averaging may reduce the impact of internal variability (Deser, Knutti, et al., 2012; Hawkins & Sutton, 2009; Lehner et al., 2020), Figs. 8 and 9 show the times series (1950-2100) of SNR for TX_x and TN_n, which are averaged over each region before the calculation of SNR (the corresponding signal and noise are in the supplementary Figs. S18-S20). For the temporal variations of median SNR over the period 1950-2014, the signal and SNR for TX_x in BEST can be within the spread of the two CMIP ensembles over some regions (Fig. 8 and Fig. S18). However, for TN_n the signal and SNR are usually outside the ranges of CMIP6 and CMIP5 at the beginning of this century (Fig. 9 and Fig. S19). Despite the influence of observational uncertainty in BEST over Australia (Deng et al., 2021), the above results suggest that the differences between the observed and simulated signal and SNR are mostly related to internal variability (Dai & Bloecker, 2019). In the study by Dai and Bloecker (2019), they concluded that comparing the trends of the observed and modelled precipitation (a variable also exhibiting relatively large variability), which can represent the signal in some studies (e.g., Gaetani et al., 2020), is not appropriate over short timescales and at local and regional scales, as the observed precipitation changes are still dominated by internal variability.

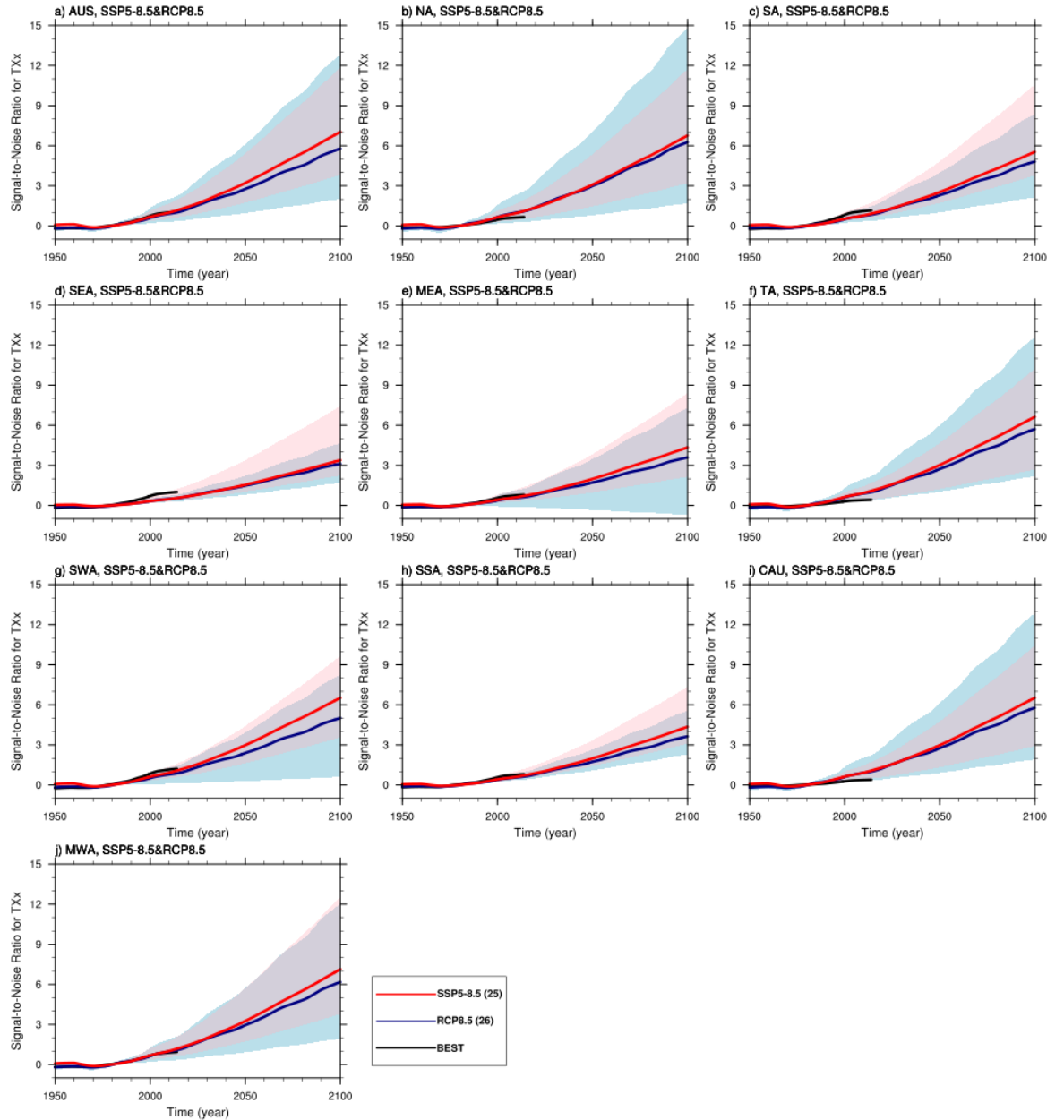


Figure 8. Time series of signal-to-noise ratio (SNR) in TXx from 1950-2100 over 10 Australian regions for BEST (black), SSP5-8.5 (red) and RCP8.5 (blue) (the number of models indicated in parentheses in the legend). Solid lines represent the multi-model medians and shading indicates the full range across the models for each experiment.

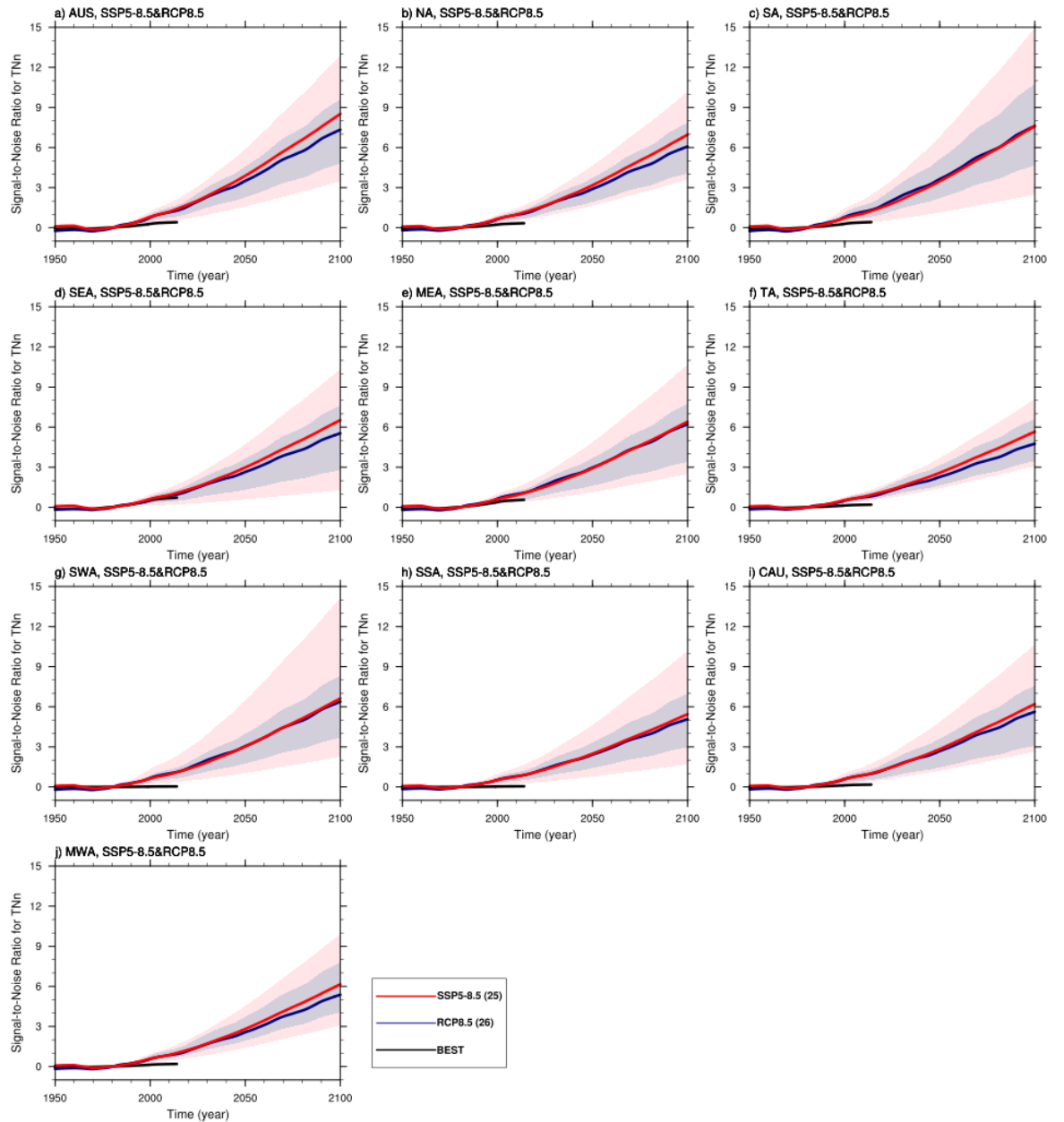


Figure 9. Same as Fig. 8, but for TNn.

Fig. 10 exhibits the spatial distributions of the multi-model median SNR for TXx and TNn under SSP5-8.5 and RCP8.5 in the year 2050, for which the signal is in Figs. S21. Under both SSP5-8.5 and RCP8.5, despite exhibiting different spatial patterns, the magnitudes of SNR for TXx and TNn are already above 1 over most Australian regions in 2050. For TXx (Fig. 10a, c), there are larger

SNR values (>2) over northwest Australia and lower SNR values (>1) over southwest regions. In contrast, the SNR for TNn (Fig. 10b, d) is more than 2 over western and central Australia and indicates lower values (>1) over tropical and southeast regions. As described in Frame et al. (2017), around mid-century, the regions exhibiting SNR > 1 suggest that there would be “unusual” climate compared to the recent climate over 1950-2005; and for TXx over northwest Australia and TNn over western and central regions, the new climate for the extremes would be “unfamiliar” (SNR > 2). Compared to RCP8.5, SSP5-8.5 in CMIP6 generally displays stronger SNR and the corresponding signal for the two indices, which is valid for other SSPs and RCPs (Figs. S22 and S23).

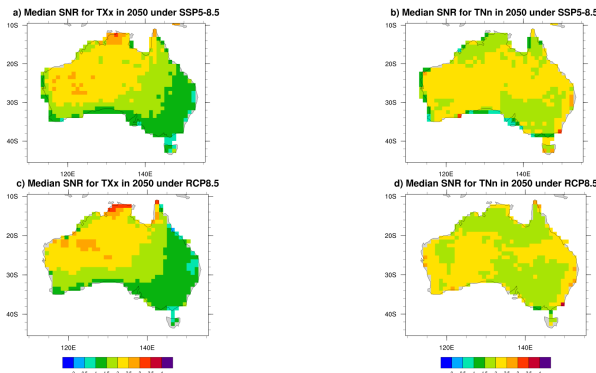


Figure 10. Median signal-to-noise ratio (SNR) for TXx and TNn under SSP5-8.5 and RCP8.5 in the year 2050. (a) SNR for TXx under SSP5-8.5 in the year 2050; (b) SNR for TNn under SSP5-8.5 in the year 2050; (c, d) same as (a) and (b), but for RCP8.5.

As for the temporal evolution of SNR (Figs. 8 and 9), in general, the multi-model medians of SNR in TXx and TNn are slightly larger in SSP5-8.5 than RCP8.5 (e.g., 3.22 under SSP5-8.5 and 2.77 under RCP8.5 in 2050 over AUS); while over some southern regions for TNn (e.g., SA, SSA, SWA), the two CMIP ensemble show higher similarity. In addition, the medians of signal and noise for the two indices are also comparable in the two scenarios (Figs. S18-S20). It is noted that the differences in signal between CMIP6 and CMIP5 in the end of the century resemble that shown in Figs. 3a and 3d, which may further imply that the regional climate sensitivity in CMIP6 and CMIP5 is comparable indicated in previous studies (Palmer et al., 2021; Seneviratne & Hauser, 2020). In terms of the inter-model spread, although the spreads of the signals for TXx and TNn in SSP5-8.5 are commonly larger than RCP8.5, in which there are more models showing stronger signal in SSP5-8.5 (Figs. S18 and S19), the ranges in noise (Fig. S20) also contribute to the uncertainty of SNR. Consequently, the relative magnitudes of SNR in SSP5-8.5 and RCP8.5 may change (e.g., Fig. 8a), compared to the signal (e.g., Fig. S18a). For example, the spread of the signal in SSP5-8.5 is slightly larger in the end of the century than RCP8.5; however, influenced by the noise, the resulting range of SNR in SSP5-8.5 becomes nar-

rower. Over the regions, the ranges of SNR for TXx are usually narrower over southern regions (e.g., SSA and SEA); in contrast, for TNn, northern regions such as TA exhibit less uncertainty for SNR and TOE. In other scenarios (Figs. S24-S27), the medians in SNR for TXx and TNn are lower, compared to SSP5-8.5&RCP8.5; and the medians in SSPs are generally still higher than that in RCPs. Also, the spreads of SNR and signal in the lower forcing pathways is generally narrower, consistent with the time series of projected changes.

To estimate the TOE for TXx and TNn, we use $\text{SNR} > 1$ and $\text{SNR} > 2$ as the thresholds (Hawkins and Sutton 2012; Frame et al. 2017; Hawkins et al. 2020) and present the spatial patterns for multi-model median TOE under SSP5-8.5 and RCP8.5 (Fig. 11). As TOE occurring at the end of the century may be a temporary change, which is considered as “pseudo-emergence”, we exclude the TOE occurring after the year 2050 (Abatzoglou et al., 2019; Diffenbaugh & Scherer, 2011; Hawkins et al., 2014; King, Donat, et al., 2015).

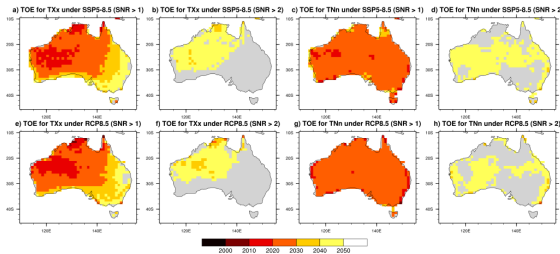


Figure 11. Median time of emergence (TOE) for TXx and TNn based on SNR thresholds under SSP5-8.5 and RCP8.5. (a) TOE for TXx under SSP5-8.5 when $\text{SNR} > 1$; (b) TOE for TXx under SSP5-8.5 when $\text{SNR} > 2$; (c, d) same as (a) and (b), but for TNn; (e-h) same as (a-d), but for RCP8.5.

Over some central and tropical parts of Australia, the multi-model median TOE in TXx for $\text{SNR} > 1$ can occur as early as the second decade of this century (2010-2020). Generally, the signal emerges earlier over northwestern region than the southeast for both thresholds (Fig. 11a, b, e and f), in which the signal emerges in 2020s for $\text{SNR} > 1$ and 2040s for $\text{SNR} > 2$, as there indicate relative smaller noise and larger signal (Figs. S17 and S21). Over the southeast regions, the TOE occurs within 2030-2050 for $\text{SNR} > 1$. In contrast, for TNn, the signal emerges from the noise in 2020s over Australia ($\text{SNR} > 1$; Fig. 11c and g);

while for $\text{SNR} > 2$, the TOE is within the fifth decade (2040-2050) over western and central regions (Fig. 11d and h). Compared to RCP8.5, the multi-model medians of TOE for TXx and TNn in CMIP6 show earlier TOE over more regions based on the threshold $\text{SNR} > 2$, implying the larger median SNR in the middle of this century as shown in Figs. 8 and 9. However, the uncertainty surrounding these TOE estimates remains large (Figs. 8 and 9). For example, for $\text{SNR} = 2$, the range (inter-model spread) of TOE for TXx over AUS can be from 2010s to 2060s (Fig. 8a). For lower scenarios, the multi-model medians of TOE commonly occur later and over smaller regions than the stronger pathways. For example, TOE ($\text{SNR} > 1$) for TNn under SSP2-4.5&RCP4.5 usually can be 10 years later over some southeast regions (Fig. S28g and k) than that shown in SSP5-8.5&RCP4.5 (Fig. 11c and g), as the signal is lower compared to that in higher pathways.

The analysis on SNR and TOE has useful implications for Australia. Under the highest-emission scenarios SSP5-8.5&RCP8.5, in which the medians of the signal for TXx are comparable, the early emergence over northwest Australia suggests that there is less time for stakeholders and policy makers to implement effective measures, compared to southeast Australia. In contrast, if under lower scenarios, the TOE for TXx can be postponed, especially for southeast regions which exhibit larger variability for TXx in the extratropics. However, the adaptation policy may change for different extremes, even under same future pathways. For TNn, the TOE ($\text{SNR} > 1$) can occur over most regions even under lower-emission scenarios; while the “unfamiliar” climate ($\text{SNR} > 2$) can be largely postponed if taking a more sustainable pathway (lower emission). It is also noted that the large uncertainty in the estimate of SNR and TOE highlights further challenges for stakeholders and policy makers.

3.3 Large Ensembles in CMIP6

Previous research has demonstrated the model uncertainty in estimating the effects of internal variability on the TXx and TNn trends, shown in LEs during 1950-2014 over Australian regions (Deng et al., 2021). Therefore, how internal variability influences the projected changes and TOE/SNR (including signal and the noise) needs further investigation. In Fig. 12, which represents the boxplots of projected changes in TXx and TNn for CanESM5-LE and MIROC6-LE over Australian regions under SSP5-8.5 and SSP1-2.6, model uncertainty for representing internal variability still exists, and the relative magnitudes of the spreads for projected changes resemble the results in Figs. 12 and 13 in Deng et al. (2021). The projected changes in TXx for MIROC6-LE span larger ranges than CanESM5-LE by a factor of ~ 3 or more over the regions, which can be larger than that in Fig. 3a. Moreover, there exhibit larger ranges of the projected changes for TXx over SEA, MEA, and SSA, and relatively narrower spreads over TA for CanESM5-LE and SWA for MIROC6-LE. For TNn, the relative magnitude for the two LEs are comparable over the regions. The different effects of internal variability for different LEs and regions complicate the assessment of the uncertainty on projected changes.

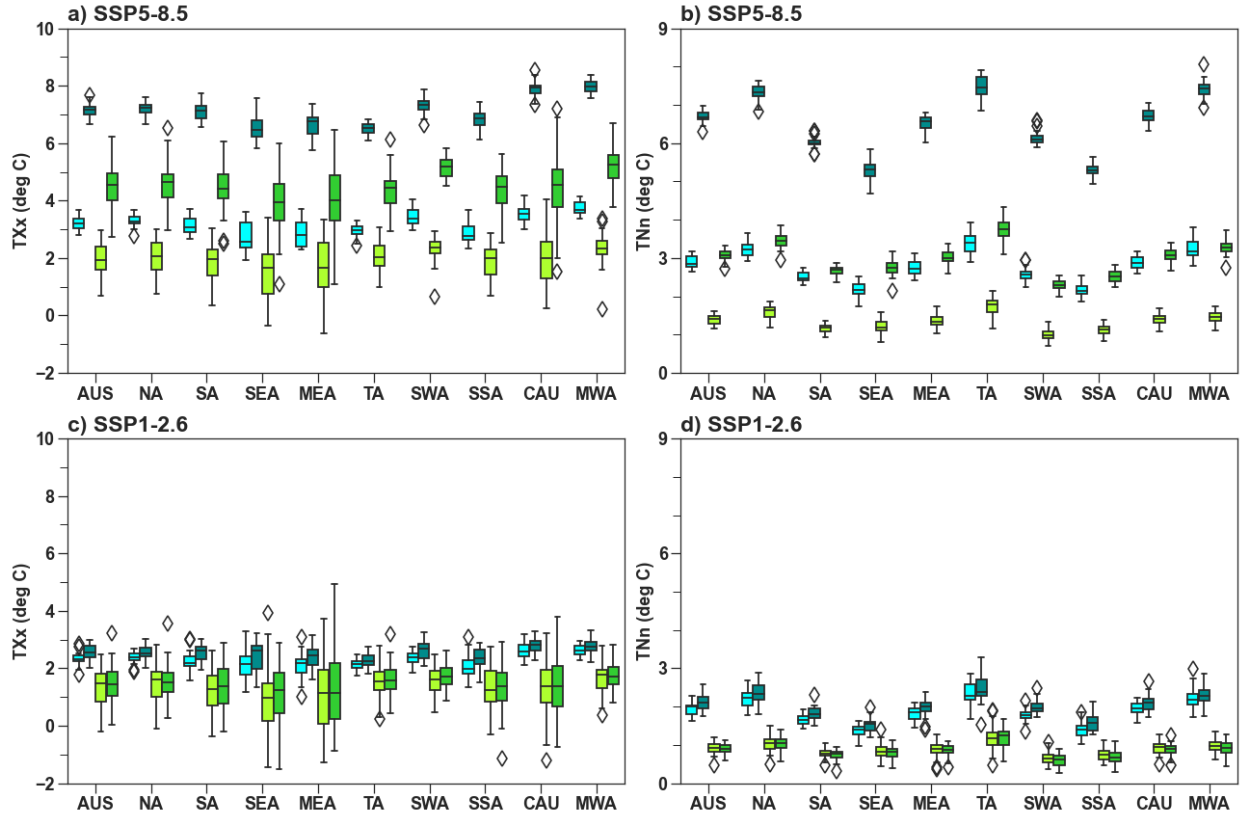


Figure 12. Boxplots of projected changes in TXx and TNn over 2071–2100 (bold color) and 2031–2060 (light color) relative to the base period 1961–1990 across 10 Australian regions, for CanESM5-LE (cyan) and MIROC6-LE (green). (a) TXx under SSP5-8.5; (b) TNn under SSP5-8.5; (c, d) same as (a, b) but for SSP1-2.6. The boxes indicate the interquartile spreads (ranges between the 25th and 75th percentiles), the black lines within the boxes are the multi-member medians, the whiskers extend to the edges of $1.5 \times$ interquartile ranges and “outliers” outside of the whiskers are denoted by diamonds.

The temporal evolution of signal and the boxplots of noise for TXx and TNn over Australian regions under SSP5-8.5 are shown in Figs. 13–15, and the resulting SNR in Figs. S29 and S30. The relative magnitudes of the ranges in signal and noise over the regions between the two LEs also resemble that for the spread of the TXx and TNn trends shown in Deng et al. (2021). This suggests that internal variability has impacts not only on the uncertainty of signal, but also on the ranges of noise, making the resulting spread of SNR (Figs. S29 and S30) wider or narrower than that for the corresponding signal (Figs. 13 and 14), which introduce further uncertainty in the ranges of TOE. Although the effects of internal variability on TXx and TNn are similar under SSP1-2.6, the

temporal evolution of the SNR and the signal for TXx and TNn stabilizes and there are narrower spreads for SNR compared to SSP5-8.5, which is due to the lower magnitude in signal under the lower scenario (Figs. S31-34).

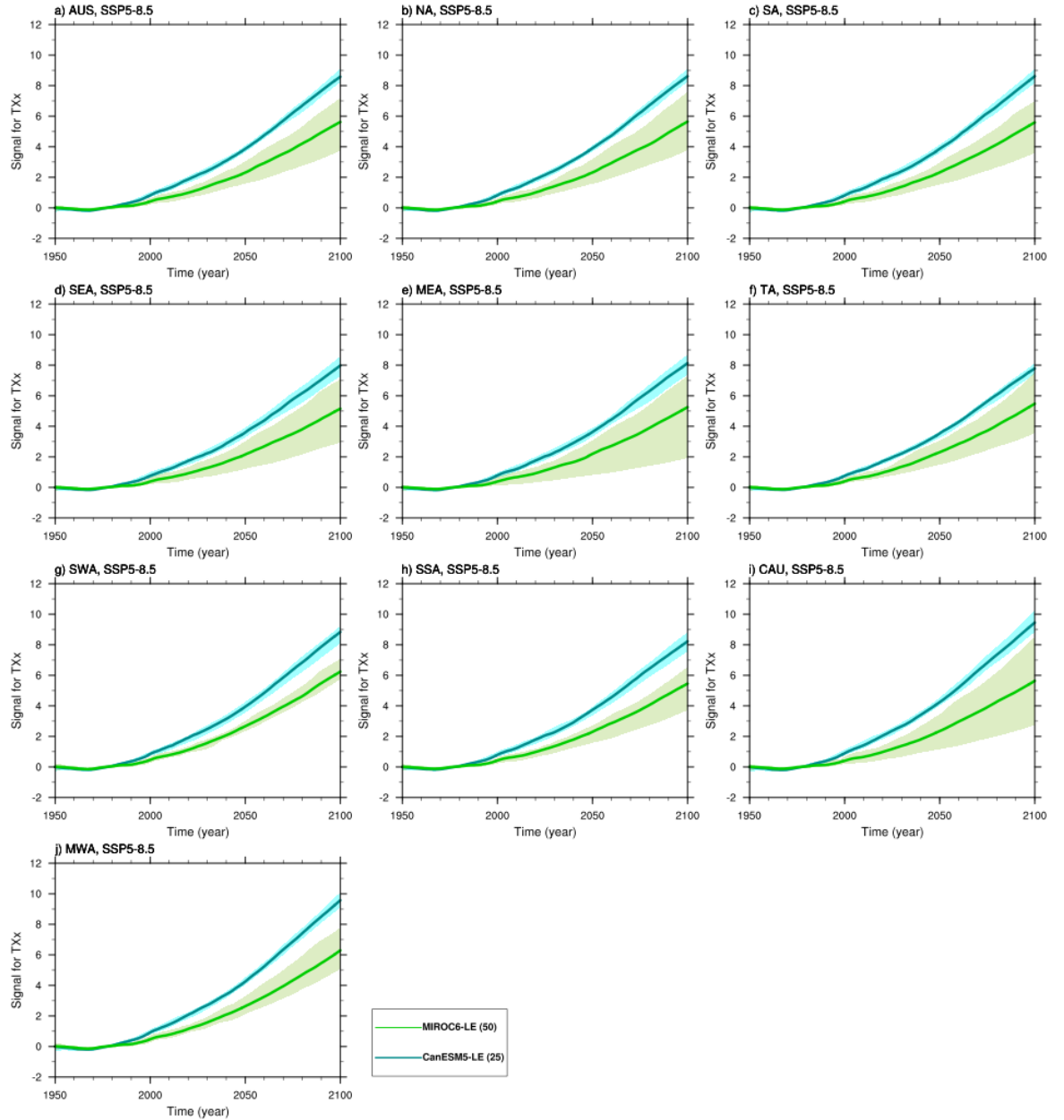


Figure 13. Time series of signal (unit: K) in TXx from 1950-2100 over 10 Australian regions under SSP5-8.5 for CanESM5-LE (cyan) and MIROC6-LE (green) (the number of members indicated in parentheses in the legend). Solid

lines represent the multi-member medians and shading indicates the full range across the members for each LE.

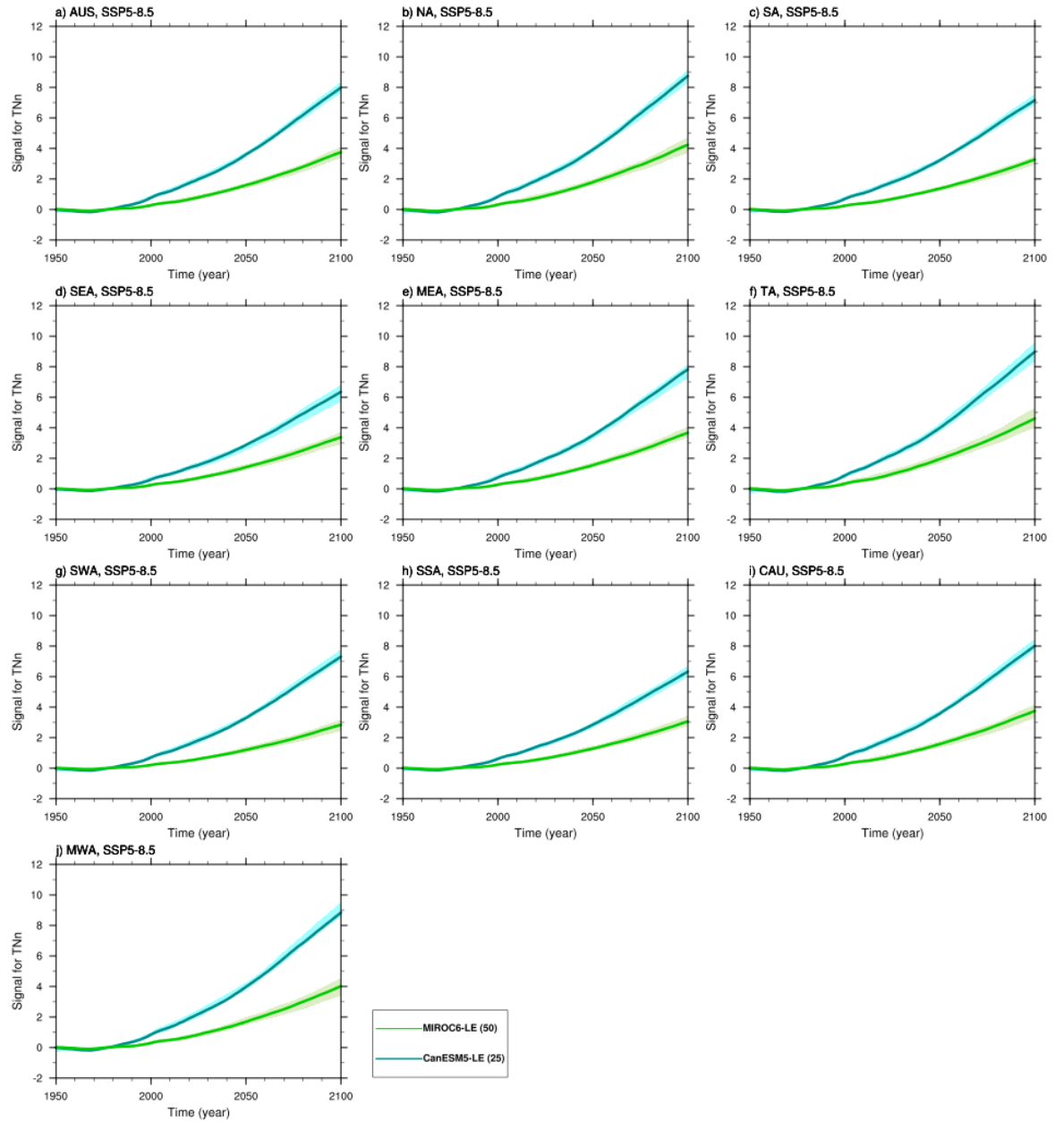


Figure 14. Same as Fig. 13, but for TNn.

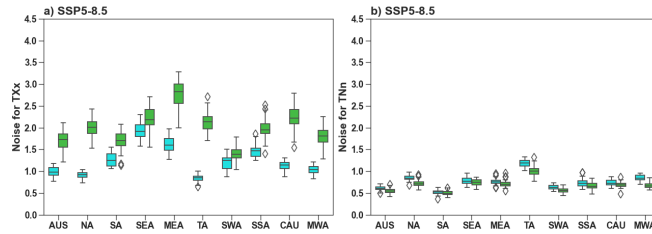


Figure 15. Boxplots of noise (unit: K) in TXx (a) and TNn (b) calculated over the period 1950-2005 across 10 Australian regions, for CanESM5-LE (cyan) and MIROC6-LE (green). The boxes indicate the interquartile spreads (ranges between the 25th and 75th percentiles), the black lines within the boxes are the multi-member medians, the whiskers extend to the edges of $1.5 \times$ interquartile ranges and “outliers” outside of the whiskers are denoted by diamonds.

4 Conclusions

In this study, we analyzed the projected changes for the temperature extremes under future scenarios (SSP1-2.6, SSP2-4.5, SSP3-7.0 and SSP5-8.5) from the Tier 1 experiment in ScenarioMIP, which is compared with RCP2.6, RCP4.5 and RCP8.5 in CMIP5. We then use an SNR framework to estimate the time when the signal of climate change for TXx and TNn emerges from the internal variability in the two CMIP ensemble. In addition, two LEs in CMIP6 are employed to estimate the effect of internal variability on the projected changes and TOE/SNR.

The projected changes for the multi-model medians of the extremes under the highest scenario show the strongest warming, and the warming for the indices under SSP3-7.0 fills the gap between SSP2-4.5 and SSP5-8.5, with SSP1-2.6 showing the least warming, especially in the end of this century. For some extreme indices (TXx, TXn, TNx, TNn, WSDI and CSDI), although the spatial patterns of warming can be different, they usually project “warm-get-warmer” pattern over Australia. As for the spread in the projections of temperature extremes, they broadly span narrower envelopes for most indices under lower scenarios in the end of this century. If we take a more sustainable pathway (SSP1-2.6), although it may take two or three decades to take effects, the narrower spreads and weaker projected changes pose relatively less challenge for adaptation decisions compared to other scenarios. Compared to other regions, TA usually shows highest warming. However, as the performance of the models over TA usually shows lower scores (Deng et al., 2021), the projected changes for the medians and the spread for the extremes may not be robust (Pierce et al., 2009),

which is also applied to other regions such as SSA and SEA.

Compared to the counterpart future pathways in CMIP5, the spread in the CMIP6 SSPs are commonly wider than RCPs; and for some extremes (e.g., TXx and TNn), the multi-model medians in SPPs are usually higher as well. This is likely caused by different forcings and higher ECS in some CMIP6 models (e.g., Fyfe et al., 2021; Palmer et al., 2021; Tebaldi et al., 2021). For example, Fyfe et al. (2021) concluded that despite the partly countervailing effect by the background stratospheric aerosols, the higher amount of CO₂ can lead to stronger warming in SSPs. In this study, we also find that for some indices (e.g., TXx), it is the models with higher ECS that usually show warmer evolution than the multi-model medians in SSP5-8.5 (not shown). To further figure out relative importance of each factor, more experiments based on CMIP6 models forced by CMIP5 RCP scenarios and/or CMIP5 models forced by CMIP6 SSP scenarios needed be conducted and added to the collection in ScenarioMIP (Fyfe et al., 2021; Tebaldi et al., 2021).

We also demonstrate that the medians of SNR for both TXx and TNn in SSPs are commonly higher than in RCPs; and the uncertainty for the SNR of TNn is wider. It is noted that the spreads of SNR for both indices decrease under lower scenarios, which confirms the benefits of lower emission future pathways. Furthermore, the large uncertainty in time of emergence (TOE) result from the inter-model spread of both signal and noise, which is consistent with Hawkins and Sutton (2012). As previous studies concluded that the statistical fit used in the SNR framework can attribute internal variability to the signals (e.g., Hawkins & Sutton, 2012; Kumar & Ganguly, 2018; Lehner et al., 2020), we further illustrate that internal variability can also influence the ranges of noise. To better isolate forced response, dynamical adjustment or LEs can be used (e.g., Lehner et al., 2020; Merrifield et al., 2020). In contrast, using the mean across the range of noise in a LE may be a more appropriate way to represent the expected noise for the model, which needs further investigation.

This study suggests that for different extreme temperature indices, the patterns for projected changes and TOE over Australia can be different, which poses large challenge for stakeholders and policymakers. A further effort is to improve the climate models in simulating the physical processes and the internal variability. Unless they are better understood and constrained, the uncertainty of projected changes and TOE will likely continue over future model generations.

Conflict of Interest

The authors declare no financial or other conflicts of interests that could have appeared to influence the work reported in this paper.

Acknowledgments

We acknowledge two anonymous reviewers for their constructive comments. We thank Edward Hawkins for feedback and comments. This research/project was undertaken with the assistance of resources and services from the National Com-

putational Infrastructure (NCI), which is supported by the Australian Government. We thank the World Climate Research Programme's Working Group on Coupled Modelling, which is responsible for CMIP and coordinated CMIP5 and CMIP6. We further acknowledge the climate modeling groups for producing and making available their model output, the Earth System Grid Federation (ESGF) for archiving the data and providing access, and the multiple funding agencies who support CMIP and ESGF. S.E.P-K. is supported by ARC grant number FT170100106 and CLEX grant number CE170100023.

Data Availability Statement

The BEST dataset is obtained from <http://berkeleyearth.org/data>, and the methodological details are provided in the references: Rohde, Muller, Jacobsen, Muller, et al. (2013) and Rohde, Muller, Jacobsen, Perlmutter, et al. (2013). The CMIP6 and CMIP5 outputs can be downloaded from the Earth System Grid Federation (<https://esgf-node.llnl.gov/search/cmip6/> and <https://esgf-node.llnl.gov/search/cmip5/>). Code for the temperature extremes in the ETCCDI indices is archived at <https://doi.org/10.5281/zenodo.4903200> (Deng, 2021).

References

<https://doi.org/10.1029/2018gl080959>
<https://doi.org/10.1016/j.wace.2017.02.001>
<https://doi.org/10.1029/2019gl084944>
[https://doi.org/10.1175/1520-0469\(1998\)055](https://doi.org/10.1175/1520-0469(1998)055)
<https://doi.org/10.1029/2019ef001421>
<https://doi.org/10.1073/pnas.1007217108>
<https://doi.org/10.1002/qj.4174>
<https://doi.org/10.2307/2286407>
<https://doi.org/10.1002/qj.776>
<https://doi.org/10.1007/s00382-018-4132-4>
<https://doi.org/10.5281/zenodo.4903200>
<https://doi.org/10.1029/2020ef001902>
<https://doi.org/10.1029/2020ef001854>
<https://doi.org/10.1038/nclimate1562>
<https://doi.org/10.1038/s41558-020-0731-2>
<https://doi.org/10.1007/s00382-010-0977-x>
<https://doi.org/10.1073/pnas.0709472105>

<https://doi.org/10.1007/s10584-011-0112-y>
<https://doi.org/10.5194/gmd-9-1937-2016>
<https://doi.org/10.1002/2014gl062018>
<https://doi.org/10.1038/nclimate3297>
<https://doi.org/10.1073/pnas.2016549118>
<https://doi.org/10.1038/s41598-020-63782-2>
<https://doi.org/10.1029/2009gl037593>
<https://doi.org/10.1029/2019ef001469>
<https://doi.org/10.1038/nature13523>
<https://doi.org/10.1029/2019gl086259>
<https://doi.org/10.1175/2009bams2607.1>
<https://doi.org/10.1029/2011gl050087>
<https://doi.org/10.1002/qj.3803>
<https://doi.org/10.22499/2.5804.003>
[https://doi.org/10.1175/1520-0477\(1996\)077](https://doi.org/10.1175/1520-0477(1996)077)
[https://doi.org/10.1175/bams-83-11-1631\(2002\)083](https://doi.org/10.1175/bams-83-11-1631(2002)083)
<https://doi.org/10.1088/1748-9326/10/9/094015>
<https://doi.org/10.1088/1748-9326/10/5/054002>
<https://doi.org/10.1007/s00382-017-3914-4>
<https://doi.org/10.5194/esd-11-491-2020>
<https://doi.org/10.1029/2019ms001940>
<https://doi.org/10.1029/2012gl053952>
<https://doi.org/10.1088/1748-9326/6/3/034009>
<https://doi.org/10.1029/2020ef001610>
<https://doi.org/10.1126/sciadv.aba1981>
<https://doi.org/10.5194/esd-11-807-2020>
<https://doi.org/10.5194/gmd-9-3461-2016>
<https://doi.org/10.1007/s00382-021-05917-3>
<https://doi.org/10.1088/1748-9326/ac1ed9>
<https://doi.org/10.1002/joc.3927>
<https://doi.org/10.1088/1748-9326/aa63fe>

<https://doi.org/10.1073/pnas.0900094106>
<https://doi.org/10.1016/j.gloenvcha.2016.05.009>
<https://doi.org/10.4172/2327-4581.1000101>
<https://doi.org/10.4172/2327-4581.1000103>
<https://doi.org/10.1029/2011jd016263>
<https://doi.org/10.1029/2019EF001474>
<https://doi.org/10.1002/jgrd.50203>
<https://doi.org/10.1002/jgrd.50188>
<https://doi.org/10.5194/acp-20-9591-2020>
<https://doi.org/10.1098/rsta.2014.0426>
<https://doi.org/10.1111/gcb.14329>
<https://doi.org/10.5194/esd-12-253-2021>
<https://doi.org/10.1007/s10584-014-1257-2>
<https://doi.org/10.1126/sciadv.aaz9549>
<https://doi.org/10.1038/nclimate2689>
<https://doi.org/10.1002/wcc.147>
<https://doi.org/10.1175/jcli3366.1>

Abatzoglou, J. T., Williams, A. P., & Barbero, R. (2019). Global emergence of anthropogenic climate change in fire weather indices. *Geophysical Research Letters*, *46*(1), 326-336. Alexander, L. V., & Arblaster, J. M. (2017). Historical and projected trends in temperature and precipitation extremes in Australia in observations and CMIP5. *Weather and Climate Extremes*, *15*, 34-56. Barnes, E. A., Hurrell, J. W., Ebert-Uphoff, I., Anderson, C., & Anderson, D. (2019). Viewing forced climate patterns through an AI Lens. *Geophysical Research Letters*, *46*(22), 13389-13398. Barsugli, J. J., & Battisti, D. S. (1998). The basic effects of atmosphere-ocean thermal coupling on midlatitude variability. *Journal of the Atmospheric Sciences*, *55*(4), 477-493. <0477:Tbeoao>2.0.Co;2Batibeniz, F., Ashfaq, M., Diffenbaugh, N. S., Key, K., Evans, K. J., Turuncoglu, U. U., et al. (2020). Doubling of U.S. population exposure to climate extremes by 2050. *Earth's Future*, *8*(4), e2019EF001421. Beaumont, L. J., Pitman, A., Perkins, S., Zimmermann, N. E., Yoccoz, N. G., & Thuiller, W. (2011). Impacts of climate change on the world's most exceptional ecoregions. *Proceedings of the National Academy of Sciences of the United States of America*, *108*(6), 2306-2311. Bell, B., Hersbach, H., Simmons, A., Berrisford, P., Dahlgren, P., Horányi, A., et al. (2021). The ERA5 global reanalysis: Preliminary extension to 1950. *Quarterly Journal of the Royal Meteorological Society*, *147*(741), 4186-4227. Cleveland, W. S. (1979). Robust locally weighted regression and smoothing scatterplots.

Journal of the American Statistical Association, 74(368), 829-836. Compo, G. P., Whitaker, J. S., Sardeshmukh, P. D., Matsui, N., Allan, R. J., Yin, X., et al. (2011). The twentieth century reanalysis project. *Quarterly Journal of the Royal Meteorological Society*, 137(654), 1-28. Dai, A., & Bloecker, C. E. (2019). Impacts of internal variability on temperature and precipitation trends in large ensemble simulations by two climate models. *Climate Dynamics*, 52(1-2), 289-306. Deng, X. (2021). Code for temperature extremes in ETCCDI indices based on the NCAR Command Language. *Zenodo*. Deng, X., Perkins-Kirkpatrick, S. E., Lewis, S. C., & Ritchie, E. A. (2021). Evaluation of extreme temperatures over Australia in the historical simulations of CMIP5 and CMIP6 models. *Earth's Future*, 9(7), e2020EF001902. Deser, C. (2020). "Certain uncertainty: The role of internal climate variability in projections of regional climate change and risk management". *Earth's Future*, 8(12), e2020EF001854. Deser, C., Knutti, R., Solomon, S., & Phillips, A. S. (2012). Communication of the role of natural variability in future North American climate. *Nature Climate Change*, 2(11), 775-779. Deser, C., Lehner, F., Rodgers, K. B., Ault, T., Delworth, T. L., DiNezio, P. N., et al. (2020). Insights from Earth system model initial-condition large ensembles and future prospects. *Nature Climate Change*, 10(4), 277-286. Deser, C., Phillips, A., Bourdette, V., & Teng, H. Y. (2012). Uncertainty in climate change projections: the role of internal variability. *Climate Dynamics*, 38(3-4), 527-546. Deutsch, C. A., Tewksbury, J. J., Huey, R. B., Sheldon, K. S., Ghalambor, C. K., Haak, D. C., et al. (2008). Impacts of climate warming on terrestrial ectotherms across latitude. *Proceedings of the National Academy of Sciences of the United States of America*, 105(18), 6668-6672. Diffenbaugh, N. S., & Scherer, M. (2011). Observational and model evidence of global emergence of permanent, unprecedented heat in the 20th and 21st centuries. *Climatic Change*, 107(3-4), 615-624. Eyring, V., Bony, S., Meehl, G. A., Senior, C. A., Stevens, B., Stouffer, R. J., et al. (2016). Overview of the Coupled Model Intercomparison Project Phase 6 (CMIP6) experimental design and organization. *Geoscientific Model Development*, 9(5), 1937-1958. Fischer, E. M., Sedláček, J., Hawkins, E., & Knutti, R. (2014). Models agree on forced response pattern of precipitation and temperature extremes. *Geophysical Research Letters*, 41(23), 8554-8562. Frame, D., Joshi, M., Hawkins, E., Harrington, L. J., & de Roiste, M. (2017). Population-based emergence of unfamiliar climates. *Nature Climate Change*, 7(6), 407-411. Fyfe, J. C., Kharin, V. V., Santer, B. D., Cole, J. N. S., & Gillett, N. P. (2021). Significant impact of forcing uncertainty in a large ensemble of climate model simulations. *Proceedings of the National Academy of Sciences of the United States of America*, 118(23), e2016549118. Gaetani, M., Janicot, S., Vrac, M., Famién, A. M., & Sultan, B. (2020). Robust assessment of the time of emergence of precipitation change in West Africa. *Scientific Reports*, 10(1), 7670. Giorgi, F., & Bi, X. (2009). Time of emergence (TOE) of GHG-forced precipitation change hot-spots. *Geophysical Research Letters*, 36(6), L06709. Grose, M. R., Narsey, S., Delage, F. P., Dowdy, A. J., Bador, M., Boschat, G., et al. (2020). Insights From CMIP6 for Australia's Future Climate. *Earth's Future*, 8(5), e2019EF001469. Hawkins, E., Anderson, B., Diffenbaugh, N., Mahlstein, I., Betts, R., Hegerl, G., et al. (2014). Uncertainties in the tim-

ing of unprecedented climates. *Nature*, 511(7507), E3-E5. Hawkins, E., Frame, D., Harrington, L., Joshi, M., King, A., Rojas, M., et al. (2020). Observed emergence of the climate change signal: From the familiar to the unknown. *Geophysical Research Letters*, 47(6), e2019GL086259. Hawkins, E., & Sutton, R. (2009). The potential to narrow uncertainty in regional climate predictions. *Bulletin of the American Meteorological Society*, 90(8), 1095-1108. Hawkins, E., & Sutton, R. (2012). Time of emergence of climate signals. *Geophysical Research Letters*, 39(1), L01702. Hersbach, H., Bell, B., Berrisford, P., Hirahara, S., Horányi, A., Muñoz-Sabater, J., et al. (2020). The ERA5 global reanalysis. *Quarterly Journal of the Royal Meteorological Society*, 146(730), 1999-2049. Intergovernmental Panel on Climate Change. (2021). *Climate Change 2021: The physical science basis. Contribution of Working Group I to the sixth assessment report of the Intergovernmental Panel on Climate Change* (V. Masson-Delmotte, P. Zhai, A. Pirani, S. L. Connors, C. Péan, S. Berger, N. Caud, Y. Chen, L. Goldfarb, M. I. Gomis, M. Huang, K. Leitzell, E. Lonnoy, J. B. R. Matthews, T. K. Maycock, T. Waterfield, O. Yelekçi, R. Yu, & B. Zhou Eds.). Cambridge, UK and New York, NY, USA: Cambridge University Press. Jones, D. A., Wang, W., & Fawcett, R. (2009). High-quality spatial climate data-sets for Australia. *Australian Meteorological and Oceanographic Journal*, 58(4), 233-248. Kalnay, E., Kanamitsu, M., Kistler, R., Collins, W., Deaven, D., Gandin, L., et al. (1996). The NCEP/NCAR 40-year reanalysis project. *Bulletin of the American Meteorological Society*, 77(3), 437-472. <0437:Thyrp>2.0.Co;2Kanamitsu, M., Ebisuzaki, W., Woollen, J., Yang, S. K., Hnilo, J. J., Fiorino, M., et al. (2002). NCEP-DOE AMIP-II Reanalysis (R-2). *Bulletin of the American Meteorological Society*, 83(11), 1631-1643. <1631:Nar>2.3.Co;2King, A. D., Donat, M. G., Fischer, E. M., Hawkins, E., Alexander, L. V., Karoly, D. J., et al. (2015). The timing of anthropogenic emergence in simulated climate extremes. *Environmental Research Letters*, 10(9), 094015. King, A. D., van Oldenborgh, G. J., Karoly, D. J., Lewis, S. C., & Cullen, H. (2015). Attribution of the record high Central England temperature of 2014 to anthropogenic influences. *Environmental Research Letters*, 10(5). Kumar, D., & Ganguly, A. R. (2018). Intercomparison of model response and internal variability across climate model ensembles. *Climate Dynamics*, 51(1-2), 207-219. Lehner, F., Deser, C., Maher, N., Marotzke, J., Fischer, E. M., Brunner, L., et al. (2020). Partitioning climate projection uncertainty with multiple large ensembles and CMIP5/6. *Earth System Dynamics*, 11(2), 491-508. Lurton, T., Balkanski, Y., Bastrikov, V., Bekki, S., Bopp, L., Braconnot, P., et al. (2020). Implementation of the CMIP6 forcing data in the IPSL-CM6A-LR model. *Journal of Advances in Modeling Earth Systems*, 12(4), e2019MS001940. Mahlstein, I., Hegerl, G., & Solomon, S. (2012). Emerging local warming signals in observational data. *Geophysical Research Letters*, 39(21), L21711. Mahlstein, I., Knutti, R., Solomon, S., & Portmann, R. W. (2011). Early onset of significant local warming in low latitude countries. *Environmental Research Letters*, 6(3), 034009. Mankin, J. S., Lehner, F., Coats, S., & McKinnon, K. A. (2020). The value of initial condition large ensembles to robust adaptation decision-making. *Earth's Future*, 8(10), e2012EF001610. Meehl, G. A., Senior, C. A., Eyring, V., Flato, G., Lamarque, J. F., Stouffer, R.

J., et al. (2020). Context for interpreting equilibrium climate sensitivity and transient climate response from the CMIP6 Earth system models. *Science Advances*, 6(26), eaba1981. Merrifield, A. L., Brunner, L., Lorenz, R., Medhaug, I., & Knutti, R. (2020). An investigation of weighting schemes suitable for incorporating large ensembles into multi-model ensembles. *Earth System Dynamics*, 11(3), 807-834. O'Neill, B. C., Tebaldi, C., van Vuuren, D. P., Eyring, V., Friedlingstein, P., Hurtt, G., et al. (2016). The Scenario Model Intercomparison Project (ScenarioMIP) for CMIP6. *Geoscientific Model Development*, 9(9), 3461-3482. Ossó, A., Allan, R. P., Hawkins, E., Shaffrey, L., & Maraun, D. (2021). Emerging new climate extremes over Europe. *Climate Dynamics*. Palmer, T. E., Booth, B. B. B., & McSweeney, C. F. (2021). How does the CMIP6 ensemble change the picture for European climate projections? *Environmental Research Letters*, 16(9), 094042. Perkins, S. E., Moise, A., Whetton, P., & Katzfey, J. (2014). Regional changes of climate extremes over Australia – A comparison of regional dynamical downscaling and global climate model simulations. *International journal of climatology*, 34(12), 3456-3478. Perkins-Kirkpatrick, S. E., Fischer, E. M., Angélil, O., & Gibson, P. B. (2017). The influence of internal climate variability on heatwave frequency trends. *Environmental Research Letters*, 12(4). Pierce, D. W., Barnett, T. P., Santer, B. D., & Gleckler, P. J. (2009). Selecting global climate models for regional climate change studies. *Proceedings of the National Academy of Sciences of the United States of America*, 106(21), 8441-8446. Riahi, K., van Vuuren, D. P., Kriegler, E., Edmonds, J., O'Neill, B. C., Fujimori, S., et al. (2017). The Shared Socioeconomic Pathways and their energy, land use, and greenhouse gas emissions implications: An overview. *Global Environmental Change*, 42, 153-168. Rohde, R., Muller, R., Jacobsen, R., Muller, E., Perlmutter, S., Rosenfeld, A., et al. (2013). A new estimate of the average Earth surface land temperature spanning 1753 to 2011. *Geoinformatics and Geostatistics: An Overview*, 1(1). Rohde, R., Muller, R., Jacobsen, R., Perlmutter, S., Rosenfeld, A., Wurtele, J., et al. (2013). Berkeley Earth temperature averaging process. *Geoinformatics and Geostatistics: An Overview*, 1(2). Santer, B. D., Mears, C., Doutriaux, C., Caldwell, P., Gleckler, P. J., Wigley, T. M. L., et al. (2011). Separating signal and noise in atmospheric temperature changes: The importance of timescale. *Journal of Geophysical Research: Atmospheres*, 116(D22), D22105. Seneviratne, S. I., & Hauser, M. (2020). Regional climate sensitivity of climate extremes in CMIP6 versus CMIP5 multi-model ensembles. *Earth's Future*, 8(9), e2019EF001474. Sillmann, J., Kharin, V. V., Zhang, X., Zwiers, F. W., & Bronaugh, D. (2013). Climate extremes indices in the CMIP5 multimodel ensemble: Part 1. Model evaluation in the present climate. *Journal of Geophysical Research: Atmospheres*, 118(4), 1716-1733. Sillmann, J., Kharin, V. V., Zwiers, F. W., Zhang, X., & Bronaugh, D. (2013). Climate extremes indices in the CMIP5 multimodel ensemble: Part 2. Future climate projections. *Journal of Geophysical Research: Atmospheres*, 118(6), 2473-2493. Smith, C. J., Kramer, R. J., Myhre, G., Alterskjær, K., Collins, W., Sima, A., et al. (2020). Effective radiative forcing and adjustments in CMIP6 models. *Atmospheric Chemistry and Physics*, 20(16), 9591-9618. Sutton, R., Suckling, E., & Hawkins, E. (2015).

What does global mean temperature tell us about local climate? *Philosophical Transactions of the Royal Society A: Mathematical, Physical and Engineering Sciences*, 373(2054), 20140426. Tan, X., Gan, T. Y., & Horton, D. E. (2018). Projected timing of perceivable changes in climate extremes for terrestrial and marine ecosystems. *Global Change Biology*, 24(10), 4696-4708. Tebaldi, C., Debeire, K., Eyring, V., Fischer, E., Fyfe, J., Friedlingstein, P., et al. (2021). Climate model projections from the Scenario Model Intercomparison Project (ScenarioMIP) of CMIP6. *Earth System Dynamics*, 12(1), 253-293. Thibeault, J. M., & Seth, A. (2014). Changing climate extremes in the Northeast United States: observations and projections from CMIP5. *Climatic Change*, 127(2), 273-287. Tokarska, K. B., Stolpe, M. B., Sippel, S., Fischer, E. M., Smith, C. J., Lehner, F., et al. (2020). Past warming trend constrains future warming in CMIP6 models. *Science Advances*, 6(12), eaaz9549. Xie, S. P., Deser, C., Vecchi, G. A., Collins, M., Delworth, T. L., Hall, A., et al. (2015). Towards predictive understanding of regional climate change. *Nature Climate Change*, 5(10), 921-930. Zhang, X., Alexander, L., Hegerl, G. C., Jones, P., Tank, A. K., Peterson, T. C., et al. (2011). Indices for monitoring changes in extremes based on daily temperature and precipitation data. *Wiley Interdisciplinary Reviews: Climate Change*, 2(6), 851-870. Zhang, X., Hegerl, G., Zwiers, F. W., & Kenyon, J. (2005). Avoiding inhomogeneity in percentile-based indices of temperature extremes. *Journal of Climate*, 18(11), 1641-1651.